Chapter 11
ADMET Prediction and Molecular Simulation of Prosopis juliflora Against Lung Cancer Protein (ATK1)

Arun Pandiyan S.
Vels Institute of Science, Technology, and Advanced Studies, India

Vivek Pazhamalai
Vels Institute of Science, Technology, and Advanced Studies, India

V. Gokul
Vels Institute of Science, Technology, and Advanced Studies, India

Ivo Romauld S.
Vels Institute of Science, Technology, and Advanced Studies, India

L. Madhumitha
Vels Institute of Science, Technology, and Advanced Studies, India

S. S. Meenambiga
https://orcid.org/0000-0002-5445-525X
Vels Institute of Science, Technology, and Advanced Studies, India

ABSTRACT

With 85% of cases being non-small-cell lung cancer (NSCLC), it is the most prevalent form of the disease. NSCLC normally develops and spreads more slowly than its counterpart, small-cell lung cancer (SCLC), which may result in a worse outcome. Adenocarcinoma, squamous cell carcinoma, and giant cell carcinoma are only a few of the subtypes of NSCLC. Each has distinct traits and approaches to treatment. Smoking continues to be a substantial risk factor for NSCLC, although it can also afflict non-smokers. This work involves development of potential anti-cancer drug from the bioactive compounds of Prosopis juliflora, an invasive shrub which is found in all over the state of Tamil Nadu. The bioactive compounds of Prosopis juliflora were screened for ADMET properties and docked against the RAC-alpha serine/threonine-protein kinase (PDB: 3o96). Then, the compound Phenol, 3,5-bis(1,1-dimethylethyl)- which has the least binding energy of -6.95 kcal/mol was used to model the firmness and dynamics of the free protein 10 picoseconds.

DOI: 10.4018/979-8-3693-1646-7.ch011

1. INTRODUCTION

1.1 Overview of Lung Cancer

Lung cancer is a malignancy characterized by the uncontrolled growth of neoplastic cells in the lung tissues. It is a heterogeneous disease with two predominant histological subtypes: non-small cell lung cancer (NSCLC), which comprises approximately 85% of all cases, and small cell lung cancer (SCLC), a more aggressive but less common variant (Schabath et al, 2019). The primary etiological factor associated with lung cancer is tobacco smoking, accounting for a substantial portion of cases. Additional risk factors include exposure to environmental carcinogens, genetic predisposition, and other occupational hazards. Lung cancer often remains clinically silent until it reaches advanced stages, at which point patients may exhibit a constellation of symptoms, including chronic cough, hemoptysis, chest pain, dyspnea, and unintentional weight loss (Travis, 2012).

Lung cancer is the leading cause of cancer-related deaths globally in both men and women, with a 14% five-year survival rate despite advancements in diagnostic techniques, and the majority of patients still present with severe disease (Bunn, 2012). Over half of lung cancer cases have no cure at diagnosis, and Stage I patients have remarkably low survival rates. Understanding molecular changes linked to poor prognosis is crucial for improving diagnosis and patient care. Genomics and proteomics have been developed to study genes and proteins in specific cell or tissue types. Differential profiling can help identify differences between tumors and normal tissues in cancer. Gene and protein expression patterns can improve lung cancer treatment by enhancing categorization and diagnostic classifiers (Gadgeel et al, 2012).

Lung cancer metastasis occurs when cancerous cells break away from the primary tumor in the lungs and enter the bloodstream or lymphatic system. These cells can travel to distant organs and tissues, where they establish new cancerous growths. The propensity of lung cancer to metastasize is attributed to several factors, including the highly vascularized nature of the lungs, which allows cancer cells to easily access the bloodstream, and the ability of lung cancer cells to evade the body's immune system (Popper, 2016). Common sites for metastasis in lung cancer include the brain, bones, liver, and adrenal glands. The brain is a frequent site due to its proximity to the lungs and the interconnected blood supply. Bone metastases can cause pain and fractures. Liver metastases can lead to impaired liver function, while adrenal gland involvement can disrupt hormone production (Riihimäki et al, 2014).

1.2 *Prosopis Juliflora*

Prosopis juliflora, an invasive plant species, is expanding rapidly in tropical and subtropical regions. As a resilient xerophyte, it provides shelter, reduces erosion, enhances micrometeorology, and provides food, feed, fuel, medicines, and cosmetics to the poor. Introduced in areas with less harsh climates and greater soil and water availability than existed in its natural environment as a result of attempts undertaken during the 19th and 20th centuries to capitalize on these characteristics of *P. juliflora* (Patnaik et al, 2017). In vitro pharmacological activities of *P. Juliflora* seed and leaf extracts include antibacterial, antifungal, and anti-inflammatory characteristics. P. juliflora is a popular traditional medicine remedy for treating inflammation, flu, sore throat, cold, measles, excrescences, dysentery, diarrhea, and wound healing. As a whole, Prosopis is known as kalpataru in India, which refers to "wonder tree" and "king of the desert," as all of the tree's parts are therapeutic (Ukande et al, 2019).

1.3 Role of ATK1 Protein in Lung Cancer

The fundamental component of cell signaling pathways that regulate cell survival and cell death is AKT/ protein kinase B (PKB) and Its resistance to apoptosis is linked to AKT activation as well as survival, growth, migration, angiogenesis and energy metabolism (Patwekar et al, 2023). AKT disruptions may be crucial in the development of tumors, according to growing research. As a result of gene amplification, mRNA overexpression, mutations resulting in constitutive phosphorylation, or the inactivation of antagonists such phosphatase and tensin homolog (PTEN), numerous publications have revealed enhanced and constitutive activation of AKT isoforms in various malignancies (Lee et al, 2011). Drug resistance to EGFR inhibitors is known to be caused by changes in this pathway, such as the PIK3CA E545K mutation or loss of PTEN. AKT's ability to convert cells and explain why cancer cells are resistant to the effects of chemotherapy and ionizing radiation are both due to its anti-apoptotic function. As a result, AKT appears to give tumor cells a growth advantage and may play a key role in regulating their growth, survival, and migration (Rao et al, 2017).

2. METHODOLOGY

2.1 Protein Preparation

The 3-dimensional structure of target protein Human ATK 1 is obtained from protein data bank (PDB ID: 3o96) (Liu et al, 2020). As the A chain of the structure contains RAC-alpha serine/threonine-protein kinase, it alone isolated and other chains and standard ligand were deleted. Removal of water molecule and addition of hydrogens and gasteiger charges to prepare protein for protein-ligand docking.

2.2 Ligand Preparation

The bioactive compounds of *Prosopis juliflora* were obtained through GC-MS (Naik et al, 2023). Then the bioactive compounds were screened for ADMET properties using ADMET predictor and SwissADME server (Diana et al, 2017) and simulation plus ADMET predictor (Ghosh et al, 2016). The compounds which satisfy the ADMET properties with better bioavailability score alone selected to dock against the target protein.

2.3 Molecular Docking

The bioactive compounds which satisfied ADMET properties were selected as ligand and docked against the Human ATK1 protein. The molecular docking process in this paper is done in Autodock4 software (Pagadala et al, 2017).

2.4 Molecular Dynamic Simulation

The protein-ligand complex which formed due to molecular docking with least binding affinity is chosen for simulation studies. Dynamics simulation is used to model the firmness and stability of protein-ligand complex. CHARM-GUI and NAMD software is used for dynamic simulation studies for this work. The

Figure 1. The 3-dimensional structure of Human ATK 1 protein

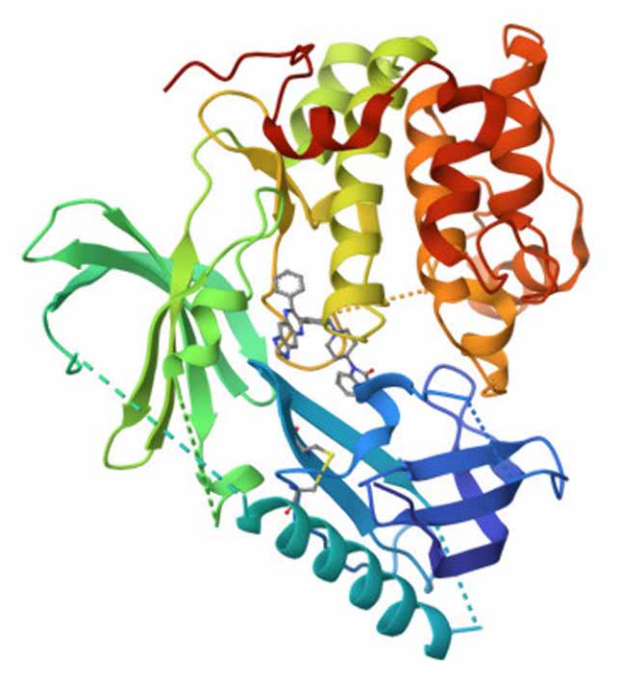

rectangular potassium chloride force field is generated and simulation is carried out for 10 picoseconds which consist of 5000 steps (Rubinstein et al, 2016).

3. RESULTS AND DISCUSSION

3.1 Protein Preparation

The three-dimensional structure of Human ATK protein 1 was retrieved from RCSB protein data bank (PDB ID: 3o96). The A chain the protein structure contains RAC-alpha serine/threonine-protein Kinase with 446 amino acid sequence length. The A chain alone isolated and prepared for docking purposes by using dockprep in the chimera software.

3.2 Ligand Preparation

The bioactive compounds of *Prosopis juliflora* were obtained through GC-MS. The compounds are retrieved from Pubchem database. Along with these compounds, reference ligand ATK 1 inhibitor which is available with the protein structure is also retrieved from the Pubchem database. The compound name and the structure of the compounds were tabulated in the Table 1.

Table 1. Bioactive compounds of Prosopis juliflora along with the reference drug

No	Name	Formula	Structure
1	Akt inhibitor VIII	C34H29N7O	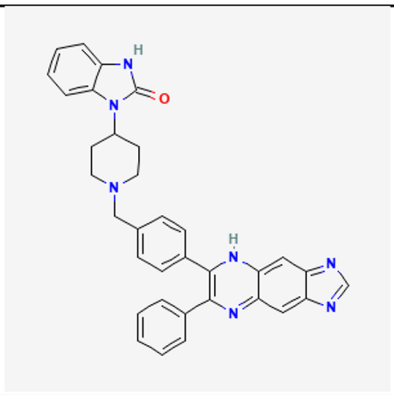
2	Ethyl Acetate	C4H8O2	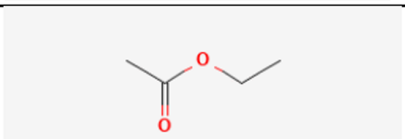
3	Butanoic acid	C4H8O2	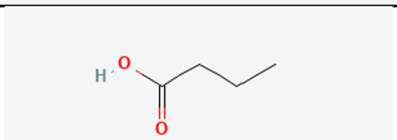
4	Acetic acid, 2-phenylethyl ester	C10H12O2	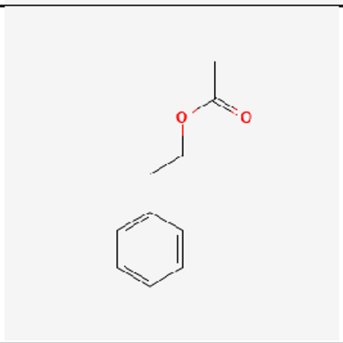
5	1-Tetradecene	C14H28	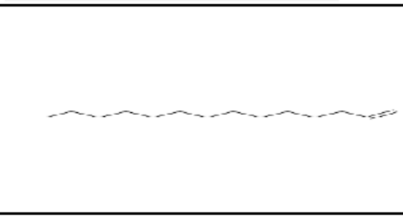

Table 1. Continued

No	Name	Formula	Structure
6	Phenol, 3,5-bis(1,1-dimethylethyl)-	C14H22O	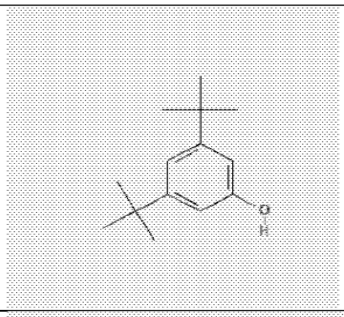
7	1-Hexadecanol	C16H34O	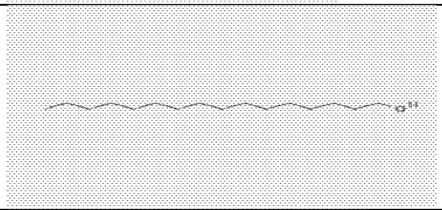
8	2-Piperidinone, N-[4-bromo-n-butyl]-	$C_9H_{16}BrNO$	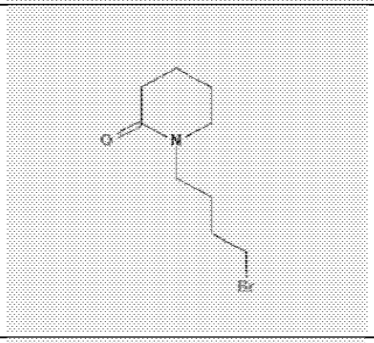
9	Phthalic acid, butyl tridec-2-yn-1-yl ester	C25H36O4	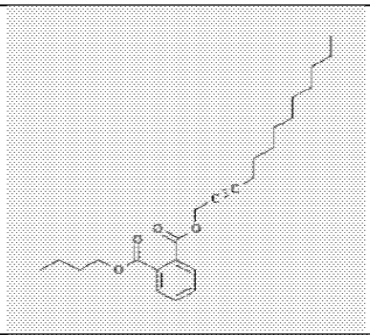
10	1-Decanol, 2-hexyl-	C16H34O	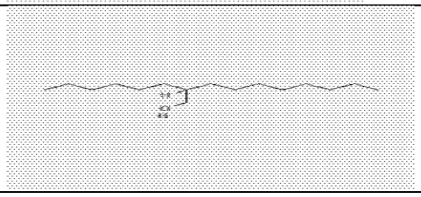

Table 1. Continued

No	Name	Formula	Structure
11	2-Methyltetracosane	C25H52	
12	7-Hexadecenal, (Z)-	C16H30O	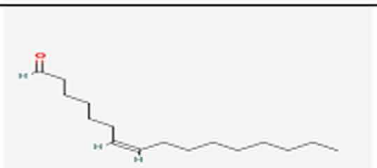
13	5-Eicosene, (E)-	C20H40	
14	1,4-Benzenedicarboxylic acid, bis(2-ethylhexyl) ester	C24H38O4	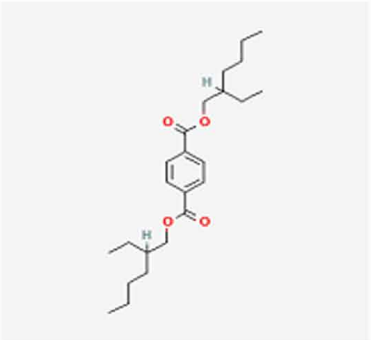
15	1-Decanol, 2-hexyl-	C16H34O	
16	Carbonic acid, eicosyl vinyl ester	C23H44O3	
17	Squalene	C30H50	
18	Heneicosane	C21H44	

3.3 ADMET Studies

3.3.1 Lipinski's Rule

The bioactive compounds of *Prosopis juliflora* was screened for Lipinski's rule of five and tabulated in Table 2. The results shows that all the compounds have satisfied the Lipinski's rule. Thus, all the compounds are orally active and have good bioavailability.

3.3.2 Absorption properties

The bioactive compounds of *Prosopis juliflora* is screened for absorption properties. The absorption properties consist of water solubility, gastrointestinal absorption, skin permeability and P-glycoprotein substrate and inhibitor. The results were tabulated in Table 3. Out of 18 compounds, only 5 compounds have higher gastrointestinal absorption with lower water solubility.

Table 2. Screening of bioactive compounds of Prosopis juliflora for Lipinski's rule of five

The Lipinski rule	The molecular weight of molecule (MW) ≤ 500.	The octanol/water partition coefficient (iLOGP = A log P) ≤ 5.	The number of hydrogen bond donors (HBDs) ≤ 5.	The number of hydrogen bond acceptors (HBAs) ≤ 10.6	The topological polar surface area (TPSA) < 40 Å^2
Ethyl Acetate	88.11	1.70	0	2	26.30
Butanoic acid	88.11	1.10	1	2	37.30
Acetic acid, 2-phenylethyl ester	164.20	2.33	0	2	26.30
1-Tetradecene	196.37	4.10	0	0	0.00
Phenol, 3,5-bis(1,1-dimethylethyl)-	206.32	2.86	1	1	20.23
1-Hexadecanol	242.44	4.41	1	1	20.23
2-Piperidinone, N-[4-bromo-n-butyl]-	234.13	2.48	0	1	20.31
Phthalic acid, butyl tridec-2-yn-1-yl ester	400.55	5.69	0	4	52.60
1-Decanol, 2-hexyl-	242.44	4.46	1	1	20.23
2-Methyltetracosane	352.68	6.78	0	0	0.00
7-Hexadecenal, (Z)-	238.41	4.02	0	1	17.07
5-Eicosene, (E)-	280.53	5.52	0	0	0.00
1,4-Benzenedicarboxylic acid, bis(2-ethylhexyl) ester	390.56	5.24	0	4	52.60
1-Decanol, 2-hexyl-	242.44	4.46	1	1	20.23
Carbonic acid, eicosyl vinyl ester	368.59	6.28	0	3	35.53
Squalene	410.72	6.37	0	0	0.00
Heneicosane	296.57	5.85	0	0	0.00

Table 3. Absorption properties of bioactive compounds of Prosopis juliflora

Compounds	Water solubility	CaCo2 permeability	GI absorption	Skin permeability	P-glycoprotein substrate	P-glycoprotein inhibitor
Ethyl Acetate	119.694	825.893	5.130	37.526	No	No (93%)
Butanoic acid	67.929	40.191	4.070	6.651	Yes	No (93%)
Acetic acid, 2-phenylethyl ester	1.921	1199.241	7.125	25.675	No (79%)	No (93%)
1-Tetradecene	0.00	1201.535	12.000	303332.066	No	Yes (59%)
Phenol, 3,5-bis(1,1-dimethylethyl)-	0.050	1047.945	9.505	2524.889	No (74%)	No (93%)
1-Hexadecanol	0.00	369.721	8.673	13230.049	No	Yes (63%)
2-Piperidinone, N-[4-bromo-n-butyl]-	1.572	740.447	6.983	22.805	No (65%)	No (64%)
Phthalic acid, butyl tridec-2-yn-1-yl ester	0.00	838.322	4.162	299.951	No (55%)	Yes (98%)
1-Decanol, 2-hexyl-	0.00	514.356	8.847	6665.926	No	Yes (60%)
2-Methyltetracosane	0.00	451.886	12.000	787103.883	No	Yes (98%)
7-Hexadecenal, (Z)-	0.001	1141.019	10.373	47367.239	No	Yes (77%)
5-Eicosene, (E)-	0.00	778.255	12.000	681093.024	No	Yes (82%)
1,4-Benzenedicarboxylic acid, bis(2-ethylhexyl) ester	0.00	834.136	5.426	821.919	No (94%)	Yes (98%)
1-Decanol, 2-hexyl-	0.00	514.356	8.847	6665.926	No	Yes (60%)
Carbonic acid, eicosyl vinyl ester	0.00	421.137	4.229	3754.613	No	Yes (98%)
Squalene	0.00	220.454	12.000	38917.742	Yes	Yes (90%)
Heneicosane	0.00	710.302	12.000	883261.419	No	Yes (98%)

3.3.3 Distribution Properties

The distribution properties of bioactive compounds of *Prosopis juliflora* is shown in Table 4. The results shows that all the compounds have higher volume of distribution rate. Thus, these compounds have extensive distribution into tissues. All the compounds have higher blood brain barrier permeability, these compounds can able to readily pass through the blood brain barrier.

3.3.4 Metabolism Properties

The outcomes of metabolism properties of bioactive compounds are shown in Table 5. To metabolize potentially harmful substances, the cytochrome p450 factor was screened and also screened for whether the compounds act as substrate or inhibitor for various hepatic enzyme. Major compounds act as both inhibitor and substrate for the CYP enzymes.

Table 4. Distribution properties of Bioactive compounds of Prosopis juliflora

Compounds	VDss human	Fraction unbound	BBB permeability
Ethyl Acetate	0.909	0.927	High (99%)
Butanoic acid	0.285	0.964	High (70%)
Acetic acid, 2-phenylethyl ester	1.072	0.755	High (99%)
1-Tetradecene	2.631	0.011	High (99%)
Phenol, 3,5-bis(1,1-dimethylethyl)-	1.912	0.086	High (99%)
1-Hexadecanol	1.698	0.011	High (96%)
2-Piperidinone, N-[4-bromo-n-butyl]-	1.172	0.735	High (99%)
Phthalic acid, butyl tridec-2-yn-1-yl ester	1.905	0.011	High (81%)
1-Decanol, 2-hexyl-	1.548	0.011	High (96%)
2-Methyltetracosane	3.139	0.011	High
7-Hexadecenal, (Z)-	2.964	0.011	High (99%)
5-Eicosene, (E)-	2.633	0.011	High (96%)
1,4-Benzenedicarboxylic acid, bis(2-ethylhexyl) ester	1.703	0.011	High (96%)
1-Decanol, 2-hexyl-	1.548	0.011	High (96%)
Carbonic acid, eicosyl vinyl ester	1.613	0.011	High (99%)
Squalene	1.825	0.011	High (93%)
Heneicosane	3.116	0.011	High (96%)

3.3.5 Excretion and Toxicity Properties

Table 6 shows the excretion and toxicity properties of bioactive compounds of Prosopis juliflora. Both rat's acute and chronic toxicity is evaluated for the compounds and tabulated. 5 compounds cause elevation in the levels of LDH hormone and 8 compounds were safe against skin sensation.

3.3. 6 Drug Likeness Properties

The drug likeness properties of the bioactive compounds were tabulated in Table 7. The properties consist of Lipinski's rule, ghose, veber, egan and muegge with bioavailability score. Each properties have their own set to rules to evaluate. A compound should satisfy either any 3 of the rules to become orally active compound. From 18 compounds, 10 compounds have satisfied at least 3 rules. Thus, those compounds only taken for the molecular docking studies.

3.4 Molecular Docking

The bioactive compounds of *Prosopis juliflora* is docked against the human ATK 1 protein along the reference ligand. The binding affinity of the docked compounds is tabulated in Table 8. The result shows that Phenol, 3,5-bis(1,1-dimethylethyl)- has least binding affinity at – 6.95 Kcal/mol followed by 1-Hexadecanol with – 5.87 Kcal/mol. The 3-dimensional and 2-dimensional interactions of Phenol, 3,5-bis(1,1-dimethylethyl)- is visualized in figure 2 and 3 respectively.

Table 5. The metabolism properties of bioactive compounds of Prosopis juliflora.

Compounds	CYP1A2 inhibitor	CYP1A2 substrate	CYP2A6 inhibitor	CYP2A6 substrate	CYP2B6 inhibitor	CYP2B6 substrate	CYP2C9 inhibitor	CYP2C9 substrate
Ethyl Acetate	No (96%)	No (65%)	No (98%)	No (74%)	Yes (52%)	Yes (47%)	No (97%)	No (99%)
Butanoic acid	No (96%)	No (75%)	No (99%)	No (74%)	No (99%)	No (98%)	No (97%)	No (89%)
Acetic acid, 2-phenylethyl ester	Yes (48%)	Yes (69%)	No (96%)	Yes (62%)	Yes (83%)	Yes (71%)	No (97%)	No (78%)
1-Tetradecene	Yes (59%)	Yes (51%)	Yes (79%)	No (86%)	Yes	Yes (67%)	No (57%)	No (86%)
Phenol, 3,5-bis(1,1-dimethylethyl)-	No (63%)	Yes (58%)	No (99%)	Yes (84%)	Yes (70%)	Yes (88%)	No (62%)	Yes (45%)
1-Hexadecanol	No (51%)	No (65%)	No (71%)	No (82%)	Yes	No (80%)	No (97%)	No (91%)
2-Piperidinone, N-[4-bromo-n-butyl]-	No (70%)	No (70%)	No (87%)	Yes (45%)	Yes (80%)	Yes (50%)	No (86%)	No (99%)
Phthalic acid, butyl tridec-2-yn-1-yl ester	Yes (67%)	No (50%)	No (96%)	No (91%)	Yes (99%)	Yes (50%)	Yes (58%)	No (89%)
1-Decanol, 2-hexyl-	No (57%)	No (63%)	No (91%)	Yes (37%)	Yes (97%)	No (65%)	No (54%)	No (86%)
2-Methyltetracosane	No (65%)	No (85%)	Yes (40%)	No (98%)	Yes	Yes (71%)	No (60%)	No (91%)
7-Hexadecenal, (Z)-	Yes (57%)	Yes (50%)	Yes (79%)	Yes (40%)	Yes	Yes (48%)	No (67%)	No (96%)
5-Eicosene, (E)-	Yes (47%)	Yes (48%)	Yes (79%)	No (98%)	Yes	Yes (88%)	No (62%)	No (84%)
1,4-Benzenedicarboxylic acid, bis(2-ethylhexyl) ester	Yes (46%)	No (54%)	No (99%)	No (94%)	Yes (97%)	Yes (71%)	Yes (60%)	No (80%)
1-Decanol, 2-hexyl-	No (57%)	No (63%)	No (91%)	Yes (37%)	Yes (97%)	No (65%)	No (54%)	No (86%)
Carbonic acid, eicosyl vinyl ester	Yes (46%)	No (58%)	No (91%)	No (98%)	Yes	No (77%)	Yes (46%)	No (94%)
Squalene	No (61%)	Yes (69%)	Yes (43%)	No	Yes	Yes	No (58%)	No
Heneicosane	No (50%)	No (70%)	Yes (64%)	No (98%)	Yes	Yes (77%)	No (60%)	No (92%)

3.5 Molecular Dynamics Simulation

The firmness and stability of Phenol, 3,5-bis(1,1-dimethylethyl)- ATK 1 protein complex Molecular dynamics simulation was carried out. The reference ligand-protein complex is also simulated under the force field for comparative studies. The RMSD graph is visualized in figure 4. The results shows that Akt inhibitor-ATK 1 protein complex has decreased RMSD compared to our target ligand-protein complex. Because it is chemically synthesized drug that have undergone various optimization. Thus, it had decreased RMSD values for each frame. Although Phenol, 3,5-bis(1,1-dimethylethyl)- ATK 1 protein complex have RMSD value nearer to 2 Å. This shows that our target ligand-protein complex is stable under the produced force field but needs some optimization. The hydrogen bonds interaction graph is visualized in figure 5. The results shows that hydrogen bonds in Phenol, 3,5-bis(1,1-dimethylethyl)- ATK 1 protein complex is higher than the reference ligand-protein complex in many frames. More the hydrogen bonds the more the stable complex. This illustrates that our target ligand-protein complex is stable and firm.

Table 6. The excretion and toxicity properties of bioactive compounds of Prosopis juliflora

Compounds	Max tolerated dose	hERG inhibitor	Oral rat acute toxicity	Oral rat chronic toxicity	Liver toxicity	Skin sensation
Ethyl Acetate	Above_3. (99%)	No	2850.305	64.782	Elevated (78%)	No (67%)
Butanoic acid	Above_3. (99%)	No	1410.873	164.643	Elevated (78%)	No (92%)
Acetic acid, 2-phenylethyl ester	Above_3. (72%)	No (51%)	3341.137	31.803	Elevated (48%)	No (84%)
1-Tetradecene	Above_3. (53%)	Yes	7282.803	351.619	Normal (65%)	Yes (95%)
Phenol, 3,5-bis(1,1-dimethylethyl)-	Above_3. (89%)	No (61%)	2754.524	235.431	Normal (83%)	Yes (74%)
1-Hexadecanol	Above_3. (86%)	No	11152.017	523.326	Normal (70%)	No (97%)
2-Piperidinone, N-[4-bromo-n-butyl]-	Above_3. (61%)	Yes (75%)	639.089	65.945	Elevated (78%)	Yes (95%)
Phthalic acid, butyl tridec-2-yn-1-yl ester	Below_3. (57%)	Yes (91%)	6298.007	213.284	Normal (94%)	No (92%)
1-Decanol, 2-hexyl-	Above_3. (89%)	No	8508.065	644.829	Normal (70%)	No (92%)
2-Methyltetracosane	Above_3.	Yes	26683.354	2361.659	Normal (83%)	Yes (58%)
7-Hexadecenal, (Z)-	Above_3. (55%)	No	7456.886	157.786	Normal (63%)	Yes (99%)
5-Eicosene, (E)-	Above_3. (55%)	Yes	15842.418	762.028	Normal (77%)	Yes (97%)
1,4-Benzenedicarboxylic acid, bis(2-ethylhexyl) ester	Above_3. (67%)	Yes (91%)	7074.887	164.365	Normal (94%)	No (92%)
1-Decanol, 2-hexyl-	Above_3. (89%)	No	8508.065	644.829	Normal (70%)	No (92%)
Carbonic acid, eicosyl vinyl ester	Above_3. (53%)	Yes	6717.048	642.898	Normal (87%)	Yes (66%)
Squalene	Above_3. (44%)	No	6730.939	579.863	Elevated	Yes
Heneicosane	Above_3.	Yes	22409.109	1142.197	Normal (83%)	Yes (63%)

4. CONCLUSION

Computer-aided drug discovery (CADD) methods have made it easier to find or anticipate a medication for a condition. This considerably reduces research time while also making important contributions to the pharmaceutical sector. CADD has sped up drug discovery to keep up with the growing global population. The development of fresh software and methodology, as well as the adoption of novel techniques, are essential for the evolution of CADD. The bioactive compounds of *Prosopis juliflora* were screened for ADMET properties and docked against the RAC-alpha serine/threonine-protein kinase (PDB: 3o96).

Table 7. The drug likeness properties of the bioactive compounds of Prosopis juliflora

Properties Compound name	Lipinski	Ghose	Veber	Egan	Muegge	Bioavailability score
Ethyl Acetate	Yes	No	Yes	Yes	No	0.55
Butanoic acid	Yes	No	Yes	Yes	No	0.85
Acetic acid, 2-phenylethyl ester	Yes	Yes	Yes	Yes	No	0.55
1-Tetradecene	Yes	Yes	No	Yes	No	0.55
Phenol, 3,5-bis(1,1-dimethylethyl)-	Yes	Yes	Yes	Yes	No	0.55
1-Hexadecanol	Yes	Yes	No	Yes	No	0.55
2-Piperidinone, N-[4-bromo-n-butyl]-	Yes	Yes	Yes	Yes	Yes	0.55
Phthalic acid, butyl tridec-2-yn-1-yl ester	Yes	No	No	No	No	0.55
1-Decanol, 2-hexyl-	Yes	Yes	No	Yes	No	0.55
2-Methyltetracosane	Yes	No	No	No	No	0.55
7-Hexadecenal, (Z)-	Yes	Yes	No	Yes	No	0.55
5-Eicosene, (E)-	Yes	No	No	No	No	0.55
1,4-Benzenedicarboxylic acid, bis(2-ethylhexyl) ester	Yes	No	No	No	No	0.55
1-Decanol, 2-hexyl-	Yes	Yes	No	Yes	No	0.55
Carbonic acid, eicosyl vinyl ester	Yes	No	No	No	No	0.55
Squalene	Yes	No	No	No	No	0.55
Heneicosane	Yes	No	No	No	No	0.55

Table 8. The binding affinity of bioactive compounds of Prosopis juliflora against ATK 1 protein

Compound name	Binding affinity energy Kcal/mol
Akt inhibitor VIII	-12.16
Ethyl Acetate	-3.57
Butanoic acid	-3.80
Acetic acid, 2-phenylethyl ester	-5.56
1-Tetradecene	-4.67
Phenol, 3,5-bis(1,1-dimethylethyl)-	-6.95
1-Hexadecanol	-5.87
2-Piperidinone, N-[4-bromo-n-butyl]-	-5.61
1-Decanol, 2-hexyl-	-5.59
7-Hexadecenal, (Z)-	-5.71
1-Decanol, 2-hexyl-	-5.50

Figure 3. The 2-dimensional interaction of Phenol, 3,5-bis(1,1-dimethylethyl)-

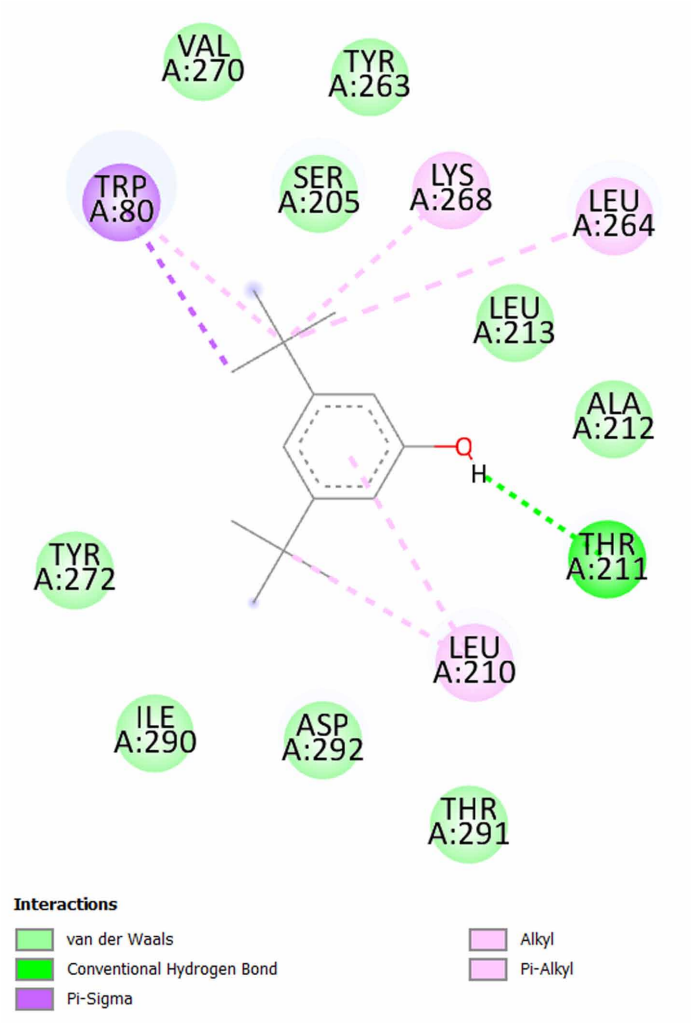

Figure 2. The 3-dimensional interaction of Phenol, 3,5-bis(1,1-dimethylethyl)-

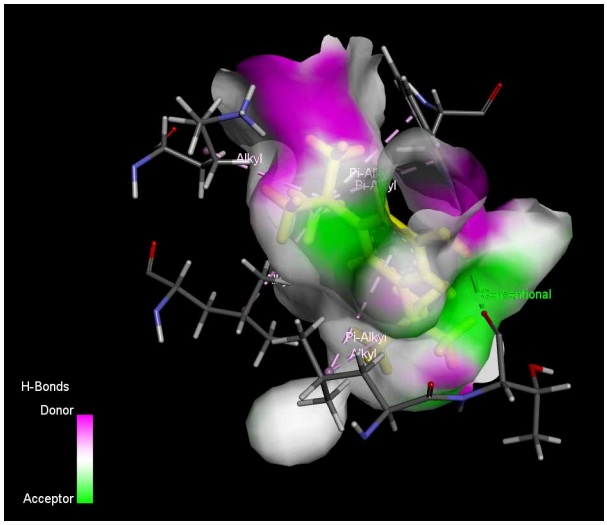

Figure 4. Root mean square deviation of Phenol, 3,5-bis(1,1-dimethylethyl)-ATK 1 complex and AKT inhibitor-ATK 1 complex

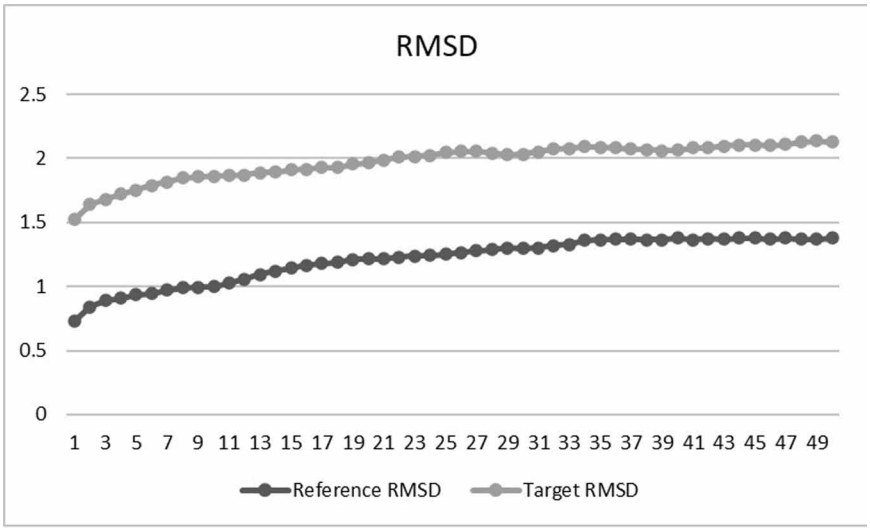

Figure 5. Hydrogen bond interactions of Phenol, 3,5-bis(1,1-dimethylethyl)-ATK 1 complex and AKT inhibitor-ATK 1 complex

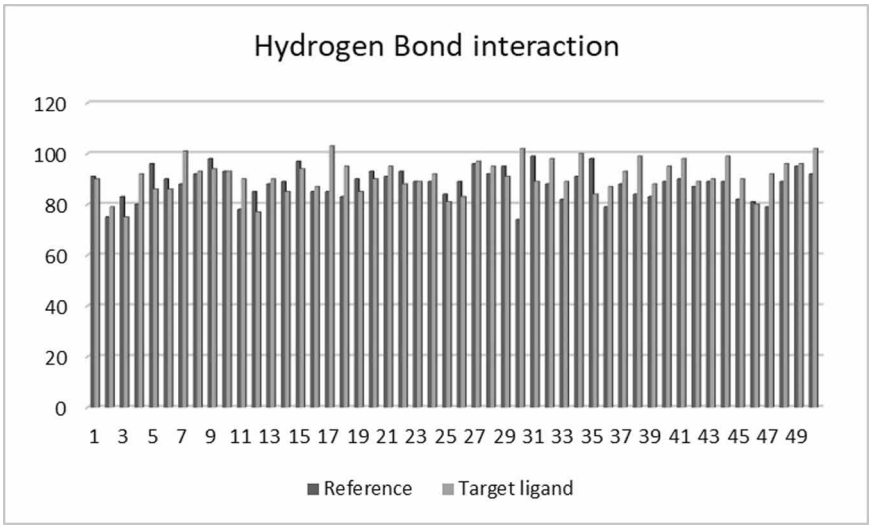

Then, the compound Phenol, 3,5-bis (1,1-dimethylethyl)- which has the least binding energy of -6.95 kcal/mol was used to model the firmness and dynamics of the free protein 10 picoseconds. Screening of bioactive compounds of *Prosopis juliflora* against the lung cancer protein shows it have a potential to inhibit the non-small-cell lung cancer. More research on this *Prosopis juliflora* will bring up the effective anti-lung cancer drug in future which may save millions of lives and more importantly it will be cost-efficient and easily available one

REFERENCES

Bunn, P. A. Jr. (2012). Worldwide overview of the current status of lung cancer diagnosis and treatment. *Archives of Pathology & Laboratory Medicine*, *136*(12), 1478–1481. doi:10.5858/arpa.2012-0295-SA PMID:23194039

Daina, A., Michielin, O., & Zoete, V. (2017). SwissADME: A free web tool to evaluate pharmacokinetics, drug-likeness and medicinal chemistry friendliness of small molecules. *Scientific Reports*, *7*(1), 42717. doi:10.1038/srep42717 PMID:28256516

Gadgeel, S. M., Ramalingam, S. S., & Kalemkerian, G. P. (2012). Treatment of lung cancer. *Radiologia Clinica*, *50*(5), 961–974. PMID:22974781

Ghosh, J., Lawless, M. S., Waldman, M., Gombar, V., & Fraczkiewicz, R. (2016). *Modeling admet. In Silico Methods for Predicting Drug Toxicity, 63-83*.

Lee, M. W., Kim, D. S., Lee, J. H., Lee, B. S., Lee, S. H., Jung, H. L., Sung, K. W., Kim, H. T., Yoo, K. H., & Koo, H. H. (2011). Roles of AKT1 and AKT2 in non-small cell lung cancer cell survival, growth, and migration. *Cancer Science*, *102*(10), 1822–1828. doi:10.1111/j.1349-7006.2011.02025.x PMID:21722267

Liu, J., Liu, Y., Zhang, J., Liu, D., Bao, Y., Chen, T., Tang, T., Lin, J., Luo, Y., Jin, Y., & Zhang, J. (2020). Indole hydrazide compound ZJQ-24 inhibits angiogenesis and induces apoptosis cell death through abrogation of AKT/mTOR pathway in hepatocellular carcinoma. *Cell Death & Disease*, *11*(10), 926. doi:10.1038/s41419-020-03108-2 PMID:33116125

Naik, N. M., Krishnaveni, M., Mahadevswamy, M., Bheemanna, M., Nidoni, U., Kumar, V., & Tejashri, K. (2023). Characterization of phyto-components with antimicrobial traits in supercritical carbon dioxide and soxhlet Prosopis juliflora leaves extract using GC-MS. *Scientific Reports*, *13*(1), 4064. doi:10.1038/s41598-023-30390-9 PMID:36906627

Pagadala, N. S., Syed, K., & Tuszynski, J. (2017). Software for molecular docking: A review. *Biophysical Reviews*, *9*(2), 91–102. doi:10.1007/s12551-016-0247-1 PMID:28510083

Patnaik, P., Abbasi, T., & Abbasi, S. A. (2017). Prosopis (Prosopis juliflora): Blessing and bane. *Tropical Ecology*, *58*(3), 455–483.

Patwekar, M., Patwekar, F., Medikeri, A., Daniyal, S., Kamal, M. A., Rather, G. A., & Sharma, R. (2023). Mechanistic insights on anticancer drugs with specific biological targets and signalling pathways. *Exploration of Medicine*, *4*(5), 637–663. doi:10.37349/emed.2023.00166

Popper, H. H. (2016). Progression and metastasis of lung cancer. *Cancer and Metastasis Reviews*, *35*(1), 75–91. doi:10.1007/s10555-016-9618-0 PMID:27018053

Rao, G., Pierobon, M., Kim, I. K., Hsu, W. H., Deng, J., Moon, Y. W., Petricoin, E. F., Zhang, Y.-W., Wang, Y., & Giaccone, G. (2017). Inhibition of AKT1 signaling promotes invasion and metastasis of non-small cell lung cancer cells with K-RAS or EGFR mutations. *Scientific Reports*, *7*(1), 7066. doi:10.1038/s41598-017-06128-9 PMID:28765579

Riihimäki, M., Hemminki, A., Fallah, M., Thomsen, H., Sundquist, K., Sundquist, J., & Hemminki, K. (2014). Metastatic sites and survival in lung cancer. *Lung Cancer (Amsterdam, Netherlands)*, *86*(1), 78–84. doi:10.1016/j.lungcan.2014.07.020 PMID:25130083

Rubinstein, R. Y., & Kroese, D. P. (2016). *Simulation and the Monte Carlo method*. John Wiley & Sons. doi:10.1002/9781118631980

Schabath, M. B., & Cote, M. L. (2019). Cancer progress and priorities: Lung cancer. *Cancer Epidemiology, Biomarkers & Prevention*, *28*(10), 1563–1579. doi:10.1158/1055-9965.EPI-19-0221 PMID:31575553

Travis, W. D. (2002). Pathology of lung cancer. *Clinics in Chest Medicine*, *23*(1), 65–81. doi:10.1016/S0272-5231(03)00061-3 PMID:11901921

Ukande, M. D., Shaikh, S., Murthy, K., & Shete, R. (2019). Review on Pharmacological potentials of Prosopis juliflora. *Journal of Drug Delivery and Therapeutics*, *9*(4-s), 755–760. doi:10.22270/jddt.v9i4-s.3372